Supporting Information

Designing Cr complexes for a neutral Fe-Cr redox flow battery

Wenqing Ruan,[abc] Jiatao Mao,[bcd], Shida Yang,[bcd] Chuan Shi,[b] Guochen Jia,[bc] Qing Chen,[*abcd]

[a]Department of Mechanical and Aerospace Engineering, HKUST, Hong Kong.

[b]Department of Chemistry, HKUST, Hong Kong.

[c]The Energy Institute, HKUST, Hong Kong.

[d]HKUST Shenzhen Research Institute, Shenzhen, China.

Correspondence should be addressed to chenqing@ust.hk.

Derivation of the screening criteria of Cr complexes

Assuming Henry's law, the equilibrium constants of the two hydrolysis reactions ($Cr^{III}(L)_n + 3OH^- \rightarrow Cr(OH)_3 + nL$ and $Cr^{II}(L)_n + 2OH^- \rightarrow Cr(OH)_2 + nL$) are respectively

$$K_1 = \frac{a_{Cr(OH)_3}[L]^n}{[Cr^{III}L_n][OH^-]^3} = \frac{K_{Cr(OH)_3}}{K_{Cr^{III}L_n}}, \quad \text{(S1)}$$

$$K_2 = \frac{a_{Cr(OH)_2}[L]^n}{[Cr^{II}L_n][OH^-]^2} = \frac{K_{Cr(OH)_2}}{K_{Cr^{II}L_n}}, \quad \text{(S2)}$$

where the square brackets are the unit-less concentrations (molarity divided by 1 M), *a*'s the activities (one for the solid hydroxides), and *K*'s the association constants. We can rearrange Eqns. 1 and 2 for

$$K_{Cr^{III}L_n} = \frac{K_{Cr(OH)_3}[Cr^{III}L_n][OH^-]^3}{a_{Cr(OH)_3}[L]^n}, \quad \text{(S3)}$$

$$K_{Cr^{II}L_n} = \frac{K_{Cr(OH)_2}[Cr^{II}L_n][OH^-]^2}{a_{Cr(OH)_2}[L]^n}. \quad \text{(S4)}$$

The neutral electrolyte sets $[OH^-] = 10^{-7}$. The complexes must dissolve at a reasonably high concentration for the RFB application., assumed 1 M. $[L]$ is usually kept low in a RFB electrolyte to maximize the solubility of the complexes. However, in the equilibria discussed here, $[L]$ has an artificially high impact that is also dependent on the value of n. To generalize the selection criteria formulated here, we compromise by assuming $[L] = 1$, meaning that a high concentration of ligands exists in the electrolyte to suppress the hydrolysis. Although it will unlikely apply in a practical RFB, the as-formulated criteria set the lower limits of $K_{Cr^{III}L}$ and $K_{Cr^{II}L}$ to be 10^9 and 10^3, respectively, given $K_{Cr(OH)_3} = 10^{17}$ and $K_{Cr(OH)_2} = 10^{30}$.

While values of $K_{Cr^{III}L}$ and $E^{0'}$ are available from the literature, $K_{Cr^{II}L}$ is rarely assessed experimentally given the instability of Cr^{II} complexes against air. So we calculate it from $K_{Cr^{III}L_n}$ and $E^{0'}$ by equilibrating the two electrochemical reactions, $Cr^{3+} + e^- \rightarrow Cr^{2+}$ and $Cr^{III}L_n + e^- \rightarrow Cr^{II}L_n$, which gives

$$E^{0'} = E^{0'}_{Cr^{3+/2+}} + \frac{RT}{F}\ln\left(\frac{K_{Cr^{II}L_n}}{K_{Cr^{III}L_n}}\right), \quad \text{(S5)}$$

where $E^{0'}_{Cr^{3+/2+}}$ is the formal potential of $Cr^{3+/2+}$ (-0.4 V vs. SHE), *R* the gas constant, *T* the temperature in Kelvin, and *F* the Faraday's constant. Rearrangement gives

$$\ln K_{Cr^{II}L_n} = \frac{F}{RT}(E^{0'} - E^{0'}_{Cr^{3+/2+}}) + \ln K_{Cr^{III}L_n}. \quad \text{(S6)}$$

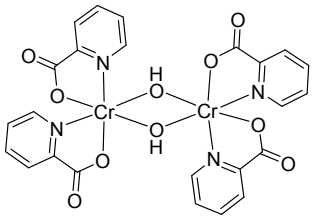

Figure S1. Molecular structures of $Cr_2(OH)_2(Pic)_4$.

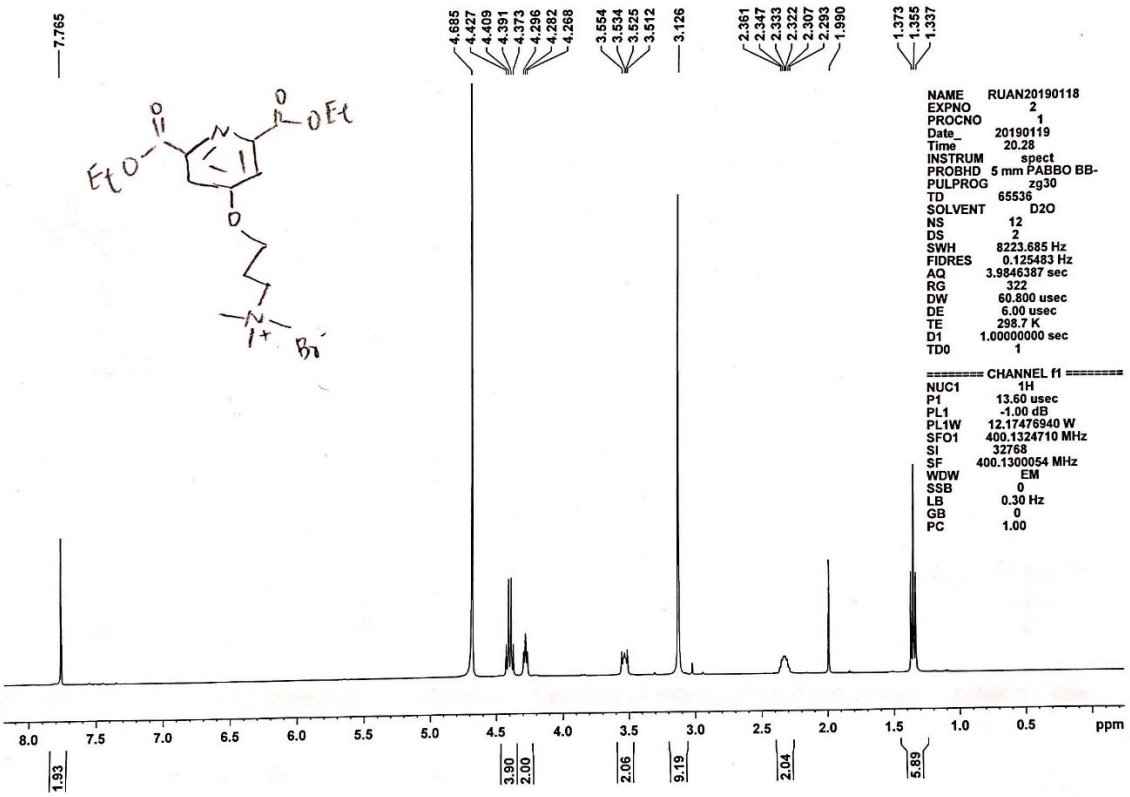

Figure S2. The ^1H NMR spectrum of 3-((2,6-bis(ethoxycarbonyl)pyridin-4-yl)oxy)-N,N,N-trimethylpropan-1-aminium bromide in D_2O at 400 MHz.

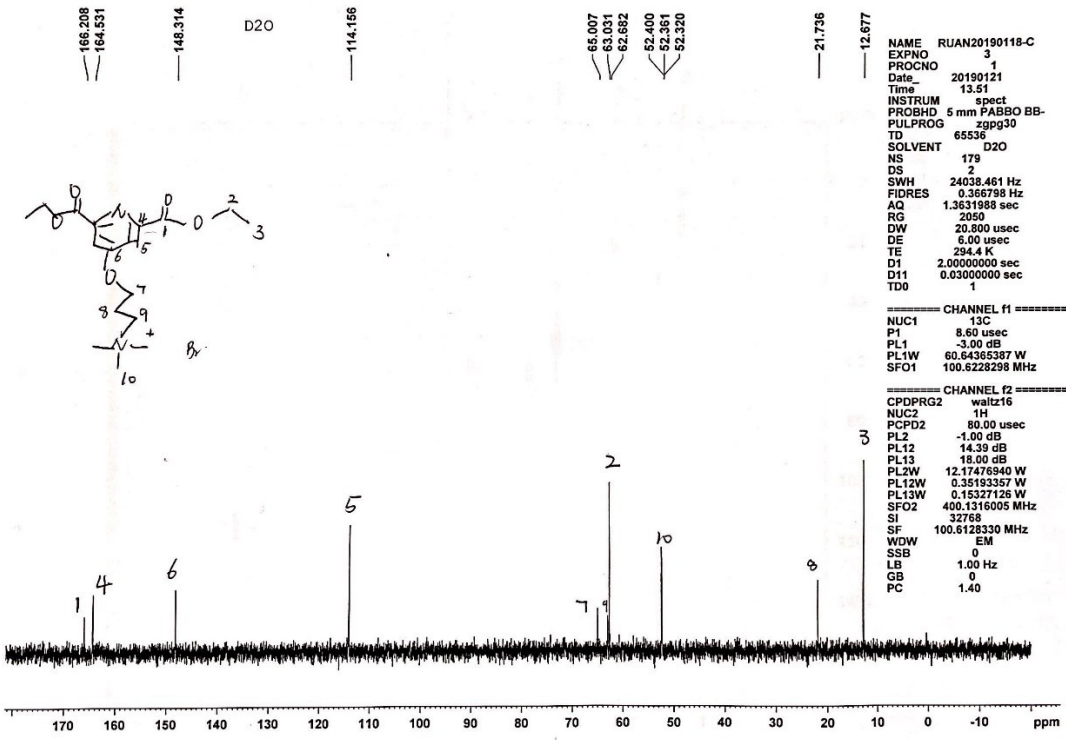

Figure S3. The ^{13}C NMR spectrum of 3-((2,6-bis(ethoxycarbonyl)pyridin-4-yl)oxy)-N,N,N-trimethylpropan-1-aminium bromide in D_2O at 100 MHz.

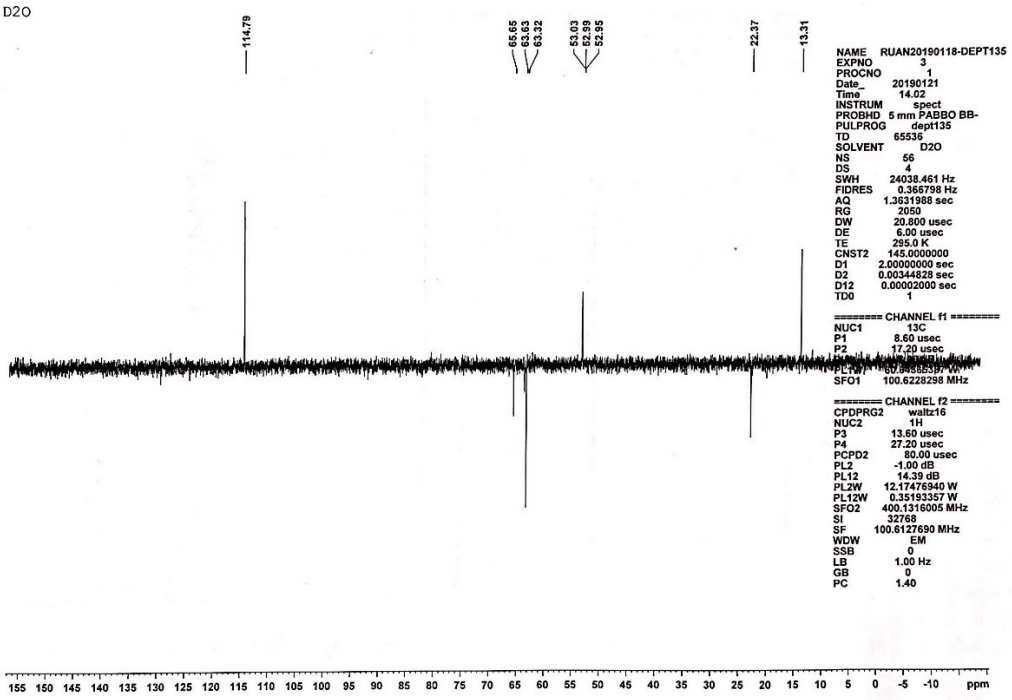

Figure S4. The ^{13}C DEPT 135 NMR spectrum of 3-((2,6-bis(ethoxycarbonyl)pyridin-4-yl)oxy)-N,N,N-trimethylpropan-1-aminium bromide in D_2O at 100 MHz.

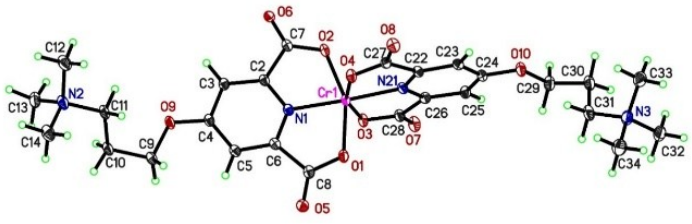

Figure S5. The X-ray crystal structure of complex [Cr(*f*-DPA)$_2$]Br (at 30% probability level of the thermal ellipsoid). CCDC 1968718 .Selected bond distances (Å) and angles (deg.): Cr(1)-O(1) 2.028(2), Cr(1)-O(2)

1.982(2), Cr(1)-O(3) 2.005(2), Cr(1)-O(4) 1.992(2), Cr(1)-N(1) 1.970(3), Cr(1)-N(21) 1.966(3), O(2)-Cr(1)-O(1) 156.64(9), O(4)-Cr(1)-O(3) 157.41(9).

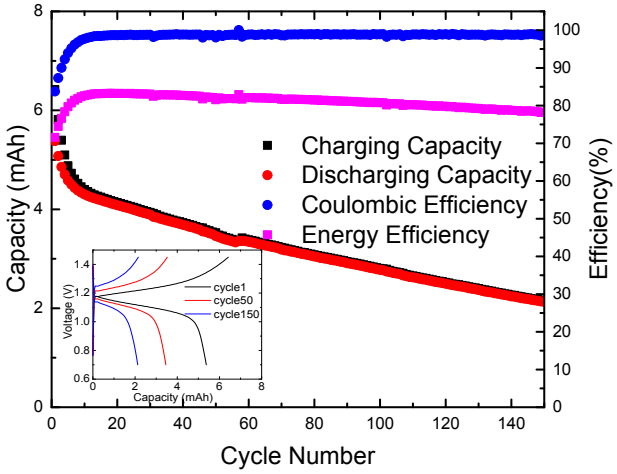

Figure S6. Capacity and efficiencies vs. cycle number of a cell tested outside a glovebox at 20 mA/cm^2. The inset shows representative voltage vs. capacity curves. The negative electrolyte contained 25 mM of [Cr(*f*-DPA)$_2$]Br. The membrane was pre-treated by first boiling in 80 ^{o}C de-ionized water for 20 minutes and then soaking in 5% hydrogen peroxide solution for 35 minutes. All other engineering parameters were the same as the cell reported in Fig. 3.

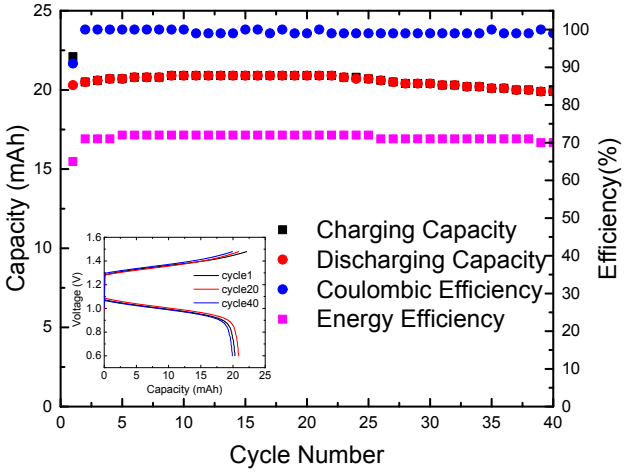

Figure S7. Capacity and efficiencies vs. cycle number from galvanostatic charging-discharging cycling at 20 mA/cm^2. The inset shows representative voltage vs. capacity curves. The engineering parameters were the same as the cell reported in Fig. 3.

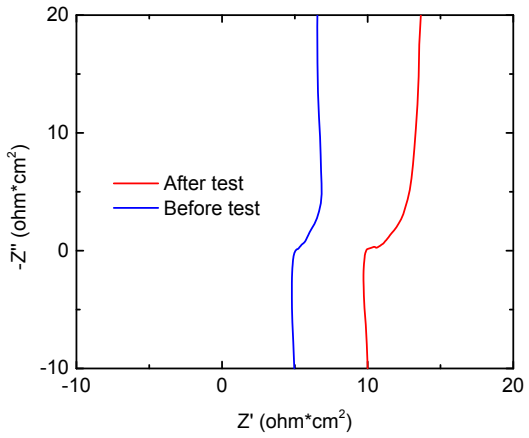

Figure S8. EIS of the ICRFB (Fig. 3) before and after the cycling test. If we naively assume linear polarization at all states of charge and a polarization resistance the same as the low frequency impedance, we can roughly estimate a change in the energy efficiency from 90% to 85% (via a method reported in *J. Electrochem. Soc., 2016, 163, A5057–A5063*), which supports the interpretation that the energy efficiency decrease is likely a result of the membrane resistance change.

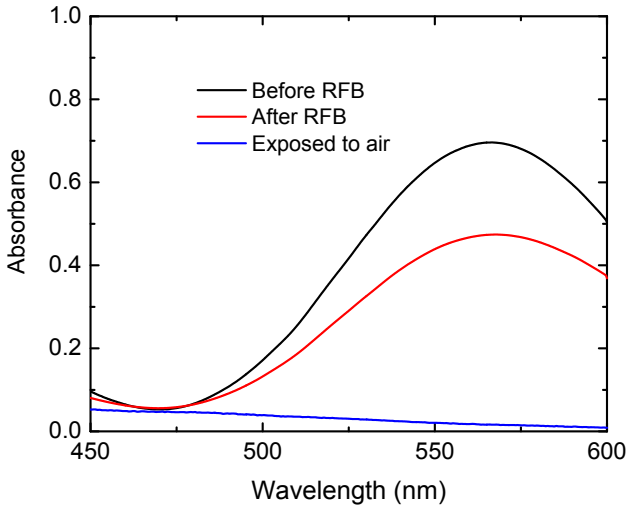

Figure S9. UV−vis absorption of [Cr(f-DPA)$_2$]Br in water before (black) and after (red) the RFB test, and after fully charged and then oxidized in air (blue). Conditions of these tests are specified in the main text and the experimental section.

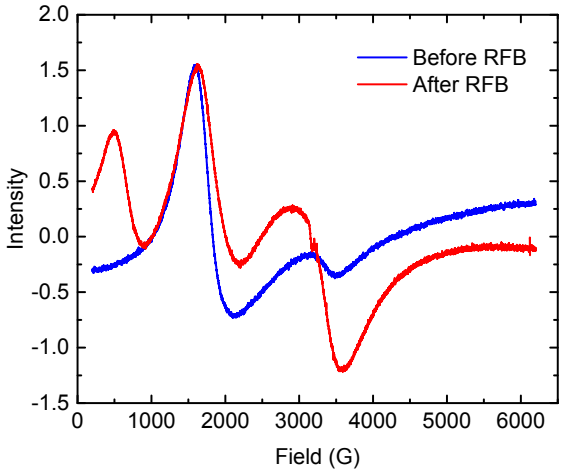

Figure S10. EPR spectra (-196 °C) of the sample [Cr(*f*-DPA)$_2$]Br in H_2O before and after the RFB test. The two peaks at 1500 and 2700 G are attributed to [Cr(*f*-DPA)$_2$]$^+$, which are present before and after the cycling test. The peak ~300 G indicates possible decomposition of the complex.

Experimental section.

Synthesis. All reactions were carried out in air condition unless otherwise specified. Diethyl 4-hydroxypyridine-2,6-dicarboxylate was prepared according to a reported procedure.[23] All other chemicals were purchased from either Aldrich or Acros Chemical Co. and used as received unless otherwise specified. ^{1}H, ^{13}C{^{1}H}, and ^{31}P{^{1}H} NMR spectra were recorded on a Bruker DPX 400 spectrometer at 400 MHz, 100 MHz and 162 MHz, respectively. All signals are reported in δ unit with references to the residual solvent resonances of the deuterated solvents for proton and carbon chemical shifts.

We added tetraethylammonium hydroxide (1.45 M water solution, 82.5 mL, 119.6 mmol) to a suspension of 2,6-Pyridinedicarboxylic acid (DPA) (10.0 g, 59.8 mmol) in H_2O (300 mL) to synthesize NEt_4[Cr(DPA)$_2$]. The reaction mixture was stirred for 15 min at room temperature to give a clear colorless solution. $CrCl_3 \cdot 6H_2O$ (8.77g, 32.9 mmol) was added and keep on stirred for 4 h at 50 °C to give a violet solution. Filtered and the filtrate was dried under vacuum, then recrystallization from H_2O to provide the NEt_4[Cr(DPA)$_2$] as a violet solid. Yield, 60% (9.19 g, 17.9 mmol).

To synthesize 3-((2,6-bis(ethoxycarbonyl)pyridin-4-yl)oxy)-N,N,N-trimethylpropan-1-aminium bromide, diethyl 4-hydroxypyridine-2,6-dicarboxylate (4.00 g, 16.7 mmol) and 3-bromo-N,N,N-trimethylpropan-1-aminium bromide (4.36g, 16.7 mmol) were dissolved in dried MeCN (100ml) under nitrogen, K_2CO_3 (3.46 g, 25.1 mmol) and KI (0.277 g, 1.67 mmol) were added. The solution was refluxed for 24 h, filtered and the filtrate was dried under vacuum, then recrystallization from DCM and Ether to provide the product as a pale solid. Yield, 65% (4.55 g, 10.8 mmol).^{1}H NMR (400 MHz, D_2O): δ 7.76 (s, 2H, Ar), 4.40 (q, J = 7.2 Hz, 4H, OCH_2CH$_3$), 4.28 (t, J = 5.6 Hz, 2H, OCH_2 CH$_2$ CH$_2$), 3.52 (m, 2H, OCH$_2$ CH$_2$ CH_2), 3.12 (s, 9H, NCH$_3$), 2.32 (m, 2H, OCH$_2$ CH_2 CH$_2$), 1.36 (t, J = 7.2 Hz, 6H, OCH$_2$CH_3),. ^{13}C{^{1}H} NMR (100 MHz, D_2O): δ 166.2 (*C*=O), 164.5 (N*C*C=O), 148.3 (*C*OCH$_2$CH$_2$CH$_2$), 114.1 (NC*C*H), 65.0 (O*C*H$_2$CH$_2$CH$_2$), 63.0 (OCH$_2$CH$_2$*C*H$_2$), 62.7 (O*C*H$_2$CH$_3$), 52.4 (m,N*C*H$_3$), 21.7 (OCH$_2$*C*H$_2$CH$_2$), 12.7 (OCH$_2$*C*H$_3$). HRMS: $[C_{17}H_{27}N_2O_5]^+$ calcd. 339.1914, found 339.1917.

[Cr(*f*-DPA)$_2$]Br was synthesized by first adding a solution of 3-((2,6-bis(ethoxycarbonyl)pyridin-4-yl)oxy)-N,N,N-trimethylpropan-1-aminium bromide (*f*-DPA) (4.0 g, 9.54 mmol) in H_2O (30 mL) to 1M KOH (19.1 mL, 19.1 mmol). The reaction mixture was reflux for 4 h under nitrogen to give a clear colorless solution. Cooled to room temperature and $CrCl_3 \cdot 6H_2O$ (1.39 g, 5.24 mmol) was added and keep on stirred for 4 h at 50 ^{o}C to give a violet solution. Filtered and the filtrate was dried under vacuum, then recrystallization from H_2O and acetone to provide the [Cr(*f*-DPA)$_2$]Br as a violet solid. Yield, 50% (1.66 g, 2.39 mmol).

Characterization. Cyclic voltammetry was performed in a three-electrode cell with a saturated calomel reference electrode and a Pt-sheet counter electrode in deaerated 1 M KCl with a BioLogic SP-300 potentiostat. UV−vis spectra were collected in a Lambda 365 ultraviolet−visible spectrophotometer (PerkinElmer). EPR spectra were measured on a Bruker ER-200D spectrometer at 9.3 GHz, modulation frequency 100 kHz, modulation amplitude 4 G.

Solubility measurements were performed via UV-Vis spectroscopy with pre-determined calibration curves. The saturated solutions were attained by dissolving the compound into water directly or by adding to this solution another salt to provide a supporting cation. A salt concentration of 0.3 M is chosen to facilitate the comparison. The concentration is high enough to precipitate out all $[Cr(DPA)_2]^-$ ions.

Flow battery assembling and testing. The battery was assembled in a typical zero-gap configuration with cell hardware from Fuel Cell Tech. It comprised two graphite endplates, two bronze current collectors, two stacks of three sheets of carbon paper electrode (SGL 39AA) on each side, and a cation exchange membrane (Nafion 212). The Nafion membranes were immersed in 0.1 M KOH solution for 2 hours, and then stored in 1 M KCl aqueous solution overnight. The membranes are rinsed with DI water before use. The active area of the electrode and the separator was 5 cm^2. A peristaltic pump (Longer, WT600-2J) was used to circulate the electrolytes through the battery at a flow rate of 60 mLmin^{-1}. 10 mL of 0.13 M of

[Cr(f-DPA)$_2$]Br + 1 M KCl aqueous solution was employed in the negative side. 20 mL of 0.15 M $K_4Fe(CN)_6$ + 0.4 M KCl solution was used in the positive side. Both sides were purged with nitrogen and then sealed before cell cycling. The battery was galvanostatically charged/discharged at room temperature on a Neware battery testing station, within a voltage window of 0.5 − 1.4 V. EIS was performed with the Bio-logic SP-300 potentiostat in the frequency range of 10 mHZ – 1 MHz.